Proceedings of the Canadian Society for Mechanical Engineering International Congress
32nd Annual Conference of the Computational Fluid Dynamics Society of Canada
Canadian Society of Rheology Symposium
CSME-CFDSC-CSR 2025
May 25–28, 2025, Montréal, Québec, Canada

STUDIES ON ADDITIVE MANUFACTURING FOR POLYMER REPAIR: MATERIAL EXTRUSION AND REVERSE ENGINEERING APPROACHES

Arjun Chandra Shekar[1,2], Marco Todescato[1,3], Jean-Philippe Leclair[1], Marco Sorgato[3], Redouane Zitoune[2,4*], Lucas A. Hof[1*]

[1]École de technologie supérieure, 1100 rue Notre-Dame Ouest, Montréal, Québec, H3C 1K3, Canada
[2]Université de Toulouse, CNRS, INSA, ISAE-SUPAERO, Mines-Albi, UPS, 3 Rue Caroline Aigle, 31400 Toulouse, France
[3]Department of Industrial Engineering, University of Padova, Via Venezia 1, 35131, Padova, Italy
[4]CINTRA CNRS/NTU/THALES, IRL 3288, Research Techno Plaza, 637553, Singapore

*lucas.hof@etsmtl.ca, redouane.zitoune@iut-tlse3.fr

Abstract—Reverse Engineering (RE) and Material Extrusion (MEX) based Additive Manufacturing (AM) present a precise and repeatable approach for polymer restoration through repair. A hemispherical additively fabricated dome shaped geometry was damaged via computer numerical control machining and digitized using 3D scanning. A reverse engineered repair patch was modeled based on scanned data and fabricated using MEX process. The patch was adhesively bonded to the parent structure. Metrological deviation analysis confirmed sub – micrometer reconstruction accuracy, with over 94% of the scanned data within ±1σ. The adhesively bonded patch showed excellent surface conformance. The findings demonstrate the feasibility of RE based additive repair as an alternative to full part replacement, and contributing to circular economy practices.

Keywords - Additive Manufacturing (AM), Material Extrusion (MEX), Polymer Repair, Reverse Engineering, Circular Economy, Polylactic Acid (PLA)

I. INTRODUCTION

Enhanced applications of polymers in modern engineering have transformed material selection due to their versatile characteristics and economic advantages [1]. Thermoplastics offer significant advantages in terms of recyclability, enhancing fabrication flexibility and circularity [2]. This property is critical within the circular economy framework, where material lifecycle and waste reduction are vital [3,4]. Polylactic Acid (PLA) has garnered considerable traction among various engineering disciplines for their ease of manufacturability and circular nature [5]. However, PLA components are susceptible to damage during handling and in-service, resulting in the need for part replacement traditionally [6]. While it seems straightforward, this approach presents challenges pertaining to economics, timeframes, impact on environment, and tooling, especially in parts demanding intricate geometries and critical functionalities [7]. With the rise in circular manufacturing principles, a paradigm shift from component replacement to repair is gradually finding adaptation across engineering domains [8]. In this context, modern reverse engineering (RE) techniques, coupled with additive manufacturing (AM), offer promising strategies for developing effective cosmetic repair methodologies. The integration of 3D scanning methods enables precise assessment of the damaged zone and digital reconstruction of the focus area, while material extrusion AM offers a viable methodology for the creation of accurate and customized repair patches [9]. However, challenges around the compatibility of printed patches matching with parent structure exist and require further investigation. Optimizing interfacial adhesion and maintaining mechanical integrity in the repaired sections ensures optimal performance of the repaired structure [10].

Current studies in material extrusion (MEX) based AM largely focus on the fabrication of polymer components rather than their restoration through repair [11]. Studies have shown the capabilities of AM to create fully functional polymer parts with customizable properties, but their direct application in repair is still underexplored [4]. Achieving geometric alignment in reverse-engineered patches, thereby aiding in strong bonding between the printed patch and the parent structure, remains a key technical challenge worth investigating. The current work focusses on establishing a structured workflow for a polymer repair methodology using MEX and RE based digital reconstruction. The method involves the fabrication of the parent part by MEX, controlled damage creation by computer numerical controlled (CNC) machining method, 3D scanning of the machined surface, modeling of the repair patch, and subsequent fabrication using MEX. The focus of choosing PLA is due to its widespread use in MEX applications, cost effectiveness, and ease of processing [12]. Through metrological evaluations after the parent – patch assembly, this study evaluates the accuracy and feasibility of using MEX in combination with 3D scanning for repairing damaged structures as part of the RE strategy. It is believed that, this work

contributes to expanding the applicability of AM in polymer restoration, enabling more efficient and scalable repair methodologies for industries adopting circular economy-oriented practices.

II. MATERIALS AND METHODS

Polymaker PolyTerra™ PLA was employed in this study, chosen for its ease of processing, biodegradability, and compatibility with MEX process [13]. The mechanical properties are listed as per Table I.

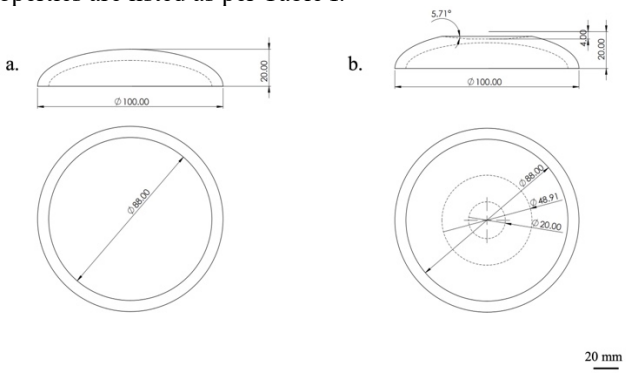

Figure 1. Specimen dimensions of parent structure: (a) before machining; (b) after machining

TABLE I. MECHANICAL PROPERTIES OF POLYTERRA™ PLA [14]

#	*Parameter*	*Value*
1.	Young's modulus	(X – Y) 1997 ± 64 MPa
		(Z) 1615 ± 54 MPa
2.	Tensile strength	(X – Y) 23.2 ± 0.5 MPa
		(Z) 12.2 ± 0.7 MPa
3.	Elongation at break	(X – Y) 27.8 ± 2.4 %
		(Z) 0.9 ± 0.1 %
4.	Bending modulus	(X – Y) 2209 ± 75 MPa
		N/A
5.	Bending strength	40.4 ± 1.1 MPa
		N/A
6.	Charpy Impact strength	6.7 ± 0.5 kJ/m^2
		N/A

To maintain consistent print quality, the filament was dried before printing process initiation at 40°C for 8 hours using a filament dehumidifier with silica gel added to absorb residual moisture. The dimensions of the parent and patch considered in this work is shown in Fig. 1.

A. Fabrication of parent structure using MEX

The parent structure was printed through MEX technique on a Bambu Lab X1E 3D printer, with slicing performed using Orca slicer v2.0 as shown in Fig. 2.

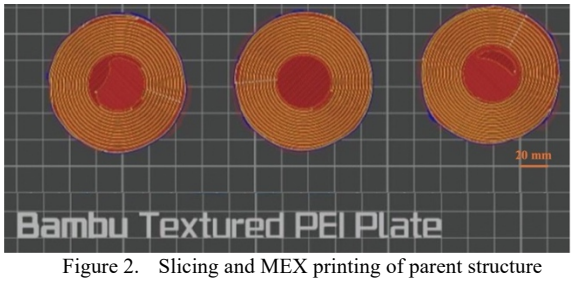

Figure 2. Slicing and MEX printing of parent structure

TABLE II. PRINTING PARAMETERS

#	*Parameter*	*Value*
1.	Nozzle diameter (mm)	0.4
2.	Layer height (mm)	0.125
3.	Infill density (%)	100
4.	Nozzle temperature (°C)	220
5.	Bed temperature (°C)	55

The CAD model was prepared, saved to *.stl* format, ensuring optimized mesh resolution before slicing. The printing parameters were maintained consistent across all specimens, as listed in Table II.

B. Controlled damage creation using CNC machining

To securely hold the printed specimen during machining, a customized MEX printed fixture was designed and fabricated using the QIDI X MAX 3D printer with standard input variables and 100% infill density. This fixture was specifically modeled and printed to conform the dome geometry of the parent structure, ensuring stability within the machining chamber. The fixture was held within the jaws of a two-part assembly as shown in Fig. 3, secured using a nut and bolt fastening.

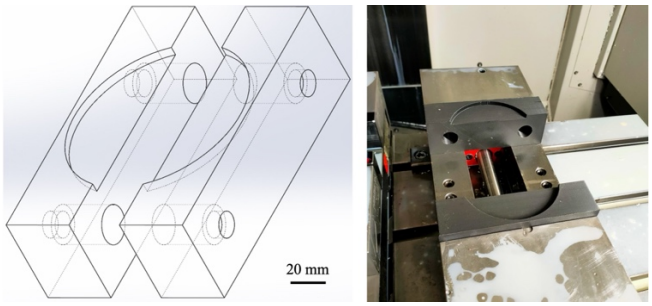

Figure 3. Fixture design and fabrication to support the parent structure during CNC machinng

For simulating real world damage scenarios, controlled material removal was performed using a Mazak Vertical Center Nexus 410A CNC machine. A ¼th inch solid carbide twist drill bit was used for machining. The machining parameters are listed in Table III.

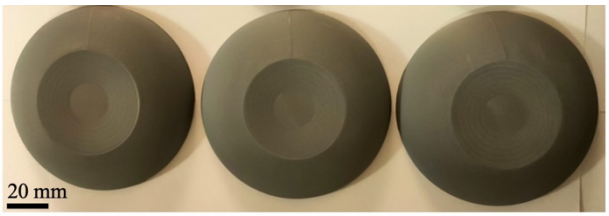

Figure 4. CNC machined parent structure

TABLE III. CNC MACHINING PARAMETERS

#	*Parameter*	*Value*
1.	Feed rate (in/min)	96
2.	Spindle speed (rpm)	12000
3.	Rough pass depth (mm)	0.3

#	***Parameter***	***Value***
4.	Finishing pass depth (mm)	0.2
5.	Lubrication	Novamet 875 cutting fluid
6.	Surface preparation	P320-grit sanding

The machining encompassed of a roughing pass and a finishing pass for removing courser and finer material with detail to achieve the final geometry of the damaged zone with the intended accuracy as shown in Fig. 4.

C. Scanning and digital reconstruction of the damaged zone

The machined parent structure was scanned using a Hexagon Absolute Arm 85, selected for high accuracy, portability, and fine scanning resolution.

The method of digital reconstruction involved *i).* 3D scanning – capturing of damaged surface from multiple angles to ensure full acquisition of the damaged zone; *ii).* Mesh optimization – cleaning the scanned data using PolyWorks Inspector to remove undesirable scanning noise; *iii).* CAD reconstruction – Importing optimized *.stl* file into SolidWorks 2024 modeling software, applying boundary surface and Boolean operations to reconstruct the patch geometry as shown in Fig. 5.

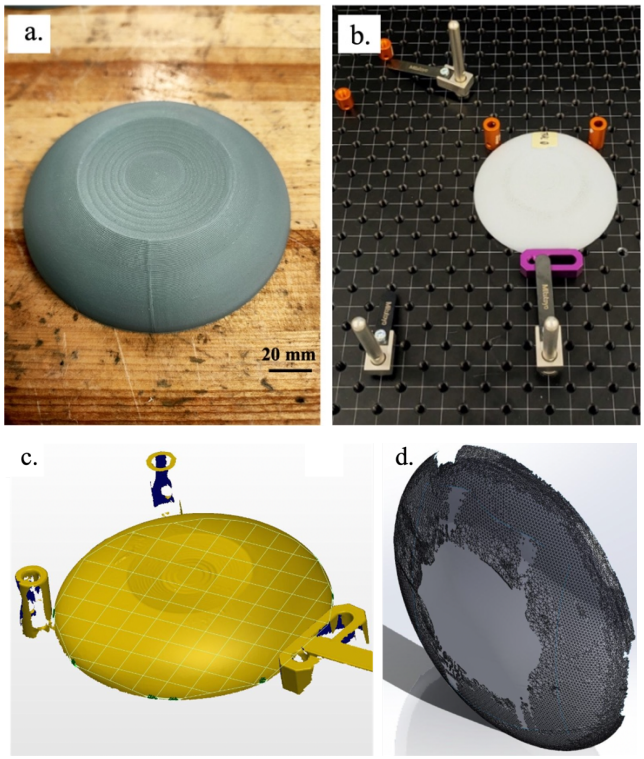

Figure 5. Scanning and digital reconstruction: (a) machined parent structure; (b) 3D scanning; (c) mesh optimization using PolyWorks Inspector; (d) boundary reconstruction using SolidWorks

The final dimensions of the machined parent structure were recorded for reference.

D. Patch fabrication using MEX

PolyWorks modeler software was used to reconstruct the patch digitally, ensuring a watertight *.stl* model before carrying the digital slicing. The printer parameters listed in Table 1 were used to maintain material consistency. Patches were printed in batches using a multi – object strategy to minimize intra – layer deformations and warpage as shown in Fig. 6.

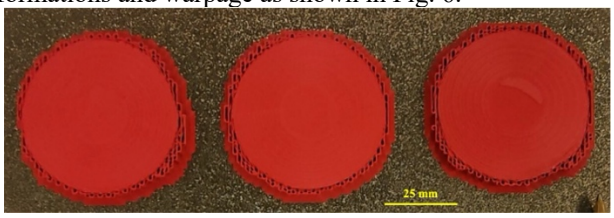

Figure 6. Additively fabricated patches after digital reconstruction of the parent structure

Consistent part orientation was ensured to carry out optimum bonding to the parent structure. The final printed patch dimensions were recorded, and they matched to the CAD designed repair patch.

E. Adhesive bonding of patch to parent structure

The printed patch was adhesively bonded to the machined parent structure using Loctite 406, a cyanoacrylate adhesive, chosen for lower viscosity levels, faster curing rates, and stronger adhesion characteristics, suitable for PLA [15].

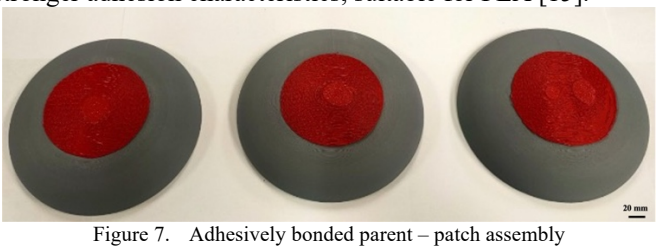

Figure 7. Adhesively bonded parent – patch assembly

The bonding process followed the surface preparation phase initially where cleaning and light sanding was undertaken. A thin, uniform layer of adhesive was further applied across the entire bonding surface. The patch was positioned accurately and naturally cured. No external pressure or clamping was done to avoid misalignment.

III. RESULTS AND DISCUSSION

The efficacy of employing RE methodologies for polymer-based repair was assessed through metrological assessments and statistical deviation studies. The analysis principally determines the evaluation of accuracy of the reconstructed patch, the repeatability of the process across multiple trials, and the overall feasibility of using AM approaches for cosmetic restoration. The findings presented in the section offer insights into how RE patch conforms to the geometry of the damaged parent structure; and how the proposed methodology ensures precise and reliable repair procedures.

1. Accuracy assessment of reverse engineering process

The accuracy of the RE procedures was studied by analyzing the deviations obtained between the reconstructed patch and the

digitally scanned parent structure. Deviation analysis was performed on the bonding interface. PolyWorks Inspector software was used for mapping the differences, with a shortest – distance method applied to obtain realistic comparisons. Three specimen assemblies of patch – parent structure were chosen for analysis, and the details are presented in Table IV. The results are in conformance that the reconstruction processes was successful in obtaining sub – micrometer accuracy, with values of mean deviation ranging within negligible range of practical repair solutions.

TABLE IV. VALIDATION OF REVERSE ENGINEERING MODELING

#	***Measurement type***	***Value***
1.	Mean deviation (µm)	0.0000067
2.	Mean standard deviation (µm)	0.0003420
3.	Maximum standard deviation (µm)	0.0004770
4.	Mean RMS value (µm)	0.0003420
5.	Maximum RMS value (µm)	0.0004770
6.	Mean Pts within +/-(1 * StdDev) (%)	94.25
7.	Mean Pts within +/-(2 * StdDev) (%)	95.65
8.	Mean Pts within +/-(3 * StdDev) (%)	96.68
9.	Mean Pts within +/-(4 * StdDev) (%)	97.83
10.	Mean Pts within +/-(5 * StdDev) (%)	98.62
11.	Mean Pts within +/-(6 * StdDev) (%)	99.26
12.	Mean max positive deviation	0.002566
13.	Absolute max positive deviation	0.003415
14.	Mean max negative deviation	-0.002893
15.	Absolute max negative deviation	-0.003902

The results show excellent reconstruction alignment, with more than 94% of the data points falling within ±1σ, validating repeatability in the scanning and reconstruction phase. As well, the mean standard deviation and the maximum standard deviation values show that most of the deviation values range around the mean value, implying lower dispersion and higher consistency in reconstruction accuracy.

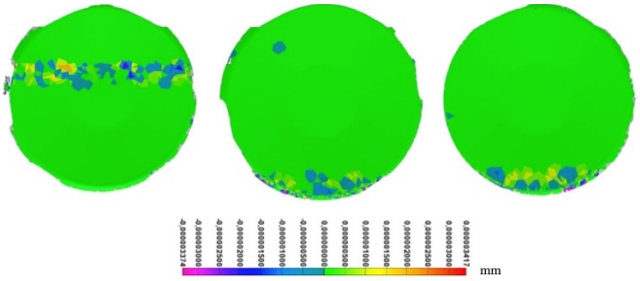

Figure 8. Validation of reverse engineering modeling: data color map highlighting the deviation between parent – patch bondline after RE phase

The mean and maximum RMS deviation values at 0.0003420 µm and 0.0004770 µm additionally confirms the minimal error, showing that no significant geometric distortions were introduced during RE modelling. The maximum deviation values are considerably small, confirms the reconstruction of patch well onto the original damaged region, ensuring a tight fit with no additional post processing operations as shown in Fig. 8. The progressive increase in deviation distribution across ±2σ to ±6σ range is reflective of the expected statistical bandwidth of the measured deviations. It implies that, most of the data points lie within the ±1σ range (94% of the points), a small percentage lie beyond and fall into the extended deviation ranges. The gradual increase suggests consistent error distribution predictions reflecting acceptable scanning and data acquisition, print and machining quality.

2. Deviation analysis of AM fabricated patch

Validation of deviations introduced during the additive manufacturing process and subsequent digitization is important to focus to obtain a realistic perspective of the process. Therefore, a comparative analysis between the pre and post printed patch was conducted, ensuring alignment with a predetermined reference coordinate system to facilitate auto alignment with original digitized parent structure. From the study, it was certain that AM process significantly contributes for higher error accumulation in comparison to the RE approach. The statistical evaluations reveal that the mean deviation was approximately 0.51 µm, while the maximum absolute deviations reached upto 488 µm, which highlights the impact of variability of AM process on accuracy. Geometric complexity of the parent structure appears to influence the magnitude of deviations, with potential sources of error accumulation emanating from the slicing, material deposition, and thermal shrinkage inherent to the AM process. From a realistic perspective, this validation is relevant as it could compromise the fir and adhesion of the AM fabricated patch when applied in cosmetic repair applications. The non – conforming regions may result in gaps or stress concentrations, affecting the overall repair quality.

3. Validation of RE and AM procedure

The combined validation of the RE modeling and AM printing process of the hemisphere showed an average mean deviation of 1.71 µm, with maximum absolute deviations closed to 490 µm as shown in Table V.

TABLE V. VALIDATION OF REVERSE ENGINEERING WITH ADDITIVE MANUFACTURING

#	***Measurement type***	***Value***
1.	Mean deviation (µm)	1.71
2.	Mean standard deviation (µm)	69.16
3.	Maximum standard deviation (µm)	97.63
4.	Mean RMS value (µm)	69.18
5.	Maximum RMS value (µm)	97.63
6.	Mean Pts within +/-(1 * StdDev) (%)	80.54
7.	Mean Pts within +/-(2 * StdDev) (%)	95.40

#	*Measurement type*	*Value*
8.	Mean Pts within +/-(3 * StdDev) (%)	98.12
9.	Mean Pts within +/-(4 * StdDev) (%)	99.19
10.	Mean Pts within +/-(5 * StdDev) (%)	99.63
11.	Mean Pts within +/-(6 * StdDev) (%)	99.79
12.	Mean max positive deviation	307.23
13.	Absolute max positive deviation	420.07
14.	Mean max negative deviation	-431.72
15.	Absolute max negative deviation	-488.29

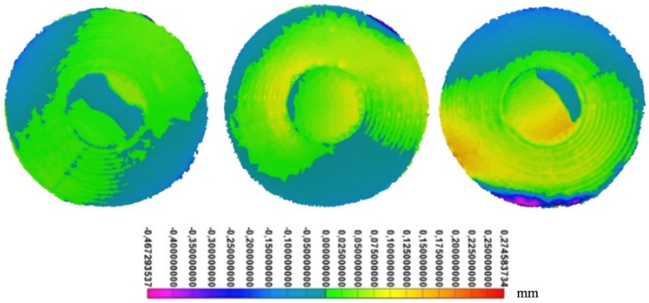

Figure 9. Validation of reverese engineering with additive manufacturing: data color map highlighting the deviation between scanned parent structure with AM fabricated patch

The results align with previous validation of AM printing, further reinforcing that the primary source of dimensional inaccuracies arise from AM process rather than RE modeling. Key observation is that geometric complexity influences error accumulation (Fig. 9), as the hemispherical dome curvature introduces additional challenges in maintaining precise alignment. The best – fit alignment procedure, despite being carried out under convergence criterion, likely resulted in minor angular misalignments, resulting to an amplified deviation. The mean root mean squared deviation and mean standard deviation around 69 µm were consistent with the errors introduced during AM. While these deviations are within acceptable tolerances, they could still be focused on finer detail with better printing tolerancing aiding to enhanced dimensional accuracy.

4. Practical application challenges and process limitations

While the current study demonstrates high accuracy and alignment, when applied in practical scenarios, the technique is susceptible for minor sources of deviation, the same are identified as follows:

- Meshing inconsistencies – Geometric distortions may arise due to surface trimming, and meshing operations, notably when the parent and patch profiles have complex curvatures. Data handling, mesh optimization play a role processing of surface data digitally.
- Variabilities due to AM process – Dimensional inconsistencies due to material variations and print inequalities give rise to deviations in dimensions. Optimum print settings to ensure negligible thermal and shrink defects are critical in maintaining dimensional integrity of the printed parts.
- Limitations of data acquisition – Inconsistencies during data acquisition and alignment during scanning affect the conformation of the patch onto the machined repair zone. Higher resolution scanning and multi – angle data acquisition is advisable for optimum scan quality.

IV. CONCLUSION

The current study demonstrates the feasibility of employing reverse engineering and material extrusion-based repair strategies for polymer structures. A detailed procedure involving 3D scanning, digital reconstruction and additive manufacturing was formulated to restore the damaged section with optimal accuracy through repair. The key findings are summarized below:

- Deviation analysis showed that more than 94% of the scanned points fell within ±1σ, confirming high precision of the digital reconstruction process.
- The mean deviation was recorded at 1.71 µm confirming that the patch required no need for post processing for integration onto the parent structure.
- Deviation analysis across three trials confirmed process stability, demonstrating minor variations in scanning and printing have no significant effect on reconstruction accuracy.
- Parent patch bonding surface exhibited uniform and continuous contact, showing minimum adhesion defects.
- With minimal manual intervention during the processing, the results strongly support the applicability of RE based repair for sustainable polymer restoration, in alignment with circular economy goals.

V. SCOPE FOR FUTURE WORK

- Mechanical testing of the repaired specimens should be carried to evaluate their structural integrity and load bearing performance.
- Surface treatment techniques could be explored to further improve adhesion strength and bond line stability during parent – patch assembly to enhance durability.

ACKNOWLEDGMENTS

The authors acknowledge the financial support of the Natural Sciences and Engineering Research Council of Canada (NSERC) under the Discovery Grant (RGPIN-2019-05973). Additional financial assistance provided by École de Technologie Supérieure's grant for international research collaborations is gratefully acknowledged as well. Gratitude is extended to Dr. Antoine Tahan for facilitating metrological instrumentation, which were critical in this research. Special thanks are also extended to Mr. Joël Grignon for his insightful discussions and technical support throughout the project. The authors further acknowledge Mr. Guillaume Villeneuve for his

technical discussions, which contributed to this work's enrichment.

REFERENCES

[1] Gil Muñoz V, Muneta LM, Carrasco-Gallego R, de Juanes Marquez J, Hidalgo-Carvajal D. Evaluation of the Circularity of Recycled PLA Filaments for 3D Printers. Applied Sciences 2020;10:8967. https://doi.org/10.3390/app10248967.

[2] Chandra Shekar A, Hadj Djilani A, Zitoune R, Toubal L, Hof LA. Effect of input variables on the mechanical properties of additively manufactured PEEK thermoplastics. Materials Today: Proceedings 2023. https://doi.org/10.1016/j.matpr.2023.09.101.

[3] Delbari SA, Hof LA. Glass waste circular economy - Advancing to high-value glass sheets recovery using industry 4.0 and 5.0 technologies. Journal of Cleaner Production 2024;462:142629. https://doi.org/10.1016/j.jclepro.2024.142629.

[4] Shekar AC, Sawalmeh A, Zitoune R, Hof LA. Optimization of surface texturing parameters in additively manufactured continuous fiber composites using abrasive waterjet technique for composite repair applications. Composites Part A: Applied Science and Manufacturing 2025;190:108698. https://doi.org/10.1016/j.compositesa.2024.108698.

[5] Kalita NK, Hakkarainen M. Integrating biodegradable polyesters in a circular economy. Current Opinion in Green and Sustainable Chemistry 2023;40:100751. https://doi.org/10.1016/j.cogsc.2022.100751.

[6] Khosravani MR, Božić Ž, Zolfagharian A, Reinicke T. Failure analysis of 3D-printed PLA components: Impact of manufacturing defects and thermal ageing. Engineering Failure Analysis 2022;136:106214. https://doi.org/10.1016/j.engfailanal.2022.106214.

[7] Joseph TM, Kallingal A, Suresh AM, Mahapatra DK, Hasanin MS, Haponiuk J, et al. 3D printing of polylactic acid: recent advances and opportunities. Int J Adv Manuf Technol 2023;125:1015–35. https://doi.org/10.1007/s00170-022-10795-y.

[8] Mejía-Moncayo C, Kenné J-P, Hof LA. On the development of a smart architecture for a sustainable manufacturing-remanufacturing system: A literature review approach. Computers & Industrial Engineering 2023;180:109282. https://doi.org/10.1016/j.cie.2023.109282.

[9] Montalti A, Ferretti P, Santi GM. A Cost-effective approach for quality control in PLA-based material extrusion 3D printing using 3D scanning. Journal of Industrial Information Integration 2024;41:100660. https://doi.org/10.1016/j.jii.2024.100660.

[10] Sourd X, Zitoune R, Hejjaji A, Salem M, Crouzeix L, Lamouche D. Multi-scale analysis of the generated damage when machining pockets of 3D woven composite for repair applications using abrasive water jet process: Contamination analysis. Composites Part A: Applied Science and Manufacturing 2020;139:106118. https://doi.org/10.1016/j.compositesa.2020.106118.

[11] Dhoonooah N, Moussaoui K, Monies F, Rubio W, Zitoune R. Challenges in Additive Manufacturing: Influence of Process Parameters on Induced Physical Properties of Printed Parts. In: Mahajan A, Devgan S, Zitoune R, editors. Additive Manufacturing of Bio-implants: Design and Synthesis, Singapore: Springer Nature; 2024, p. 1–31. https://doi.org/10.1007/978-981-99-6972-2_1.

[12] Venkatesh C, Fuenmayor E, Doran P, Major I, Lyons JG, Devine DM. Additive manufacturing of PLA/HNT nanocomposites for biomedical applications. Procedia Manufacturing 2019;38:17–24. https://doi.org/10.1016/j.promfg.2020.01.003.

[13] Zhai C, Wang J, (Paul) Tu Y, Chang G, Ren X, Ding C. Robust optimization of 3D printing process parameters considering process stability and production efficiency. Additive Manufacturing 2023;71:103588. https://doi.org/10.1016/j.addma.2023.103588.

[14] PolyTerra-PLA_TDS_V5.3.pdf n.d.

[15] LOCTITE® 406 n.d. https://www.henkel-adhesives.com/ca/en/product/instant-adhesives/loctite_4060.html (accessed February 10, 2025).